# SPATIAL AND TEMPORAL VARIATIONS OF THE KINEMATIC CHARACTERISTICS IN THE PROPAGATION OF ATMOSPHERIC STATIONARY WAVES

*Wu Guoxiong* (吴国雄), *Chen Biao* (陈 彪)* and *Wu Zhengxian* (吴正贤)

LASG**, Institute of Atmospneric Physics, Academia Sinica, Beijing

Received October 9, 1989

ABSTRACT

Time-mean global general circulation data are employed to analyze the temporal and spatial variations of the meridional gradient of zonal mean potential vorticity, the critical wavenumber $n_s$ for horizontal wave-propagation, and the critical wavenumber $K_c$ for vertical wave-propagation. Thereby the kinematic characteristics in the propagation of atmospheric stationary waves and their annual variations are studied. Results show that in the troposphere $n_s$ and $K_c$ usually decrease with the increase of either latitude or altitude. Synoptic and near-resonant Rossby waves could be trapped during their upward and meridional propagations. These characteristics possess prominent annual variations, especially in the Northern Hemisphere. It is found that the spatial and temporal variations of these kinematic characteristics are in good agreement with those of the atmospheric wave patterns.

## I. INTRODUCTION

Since the theories concerning the vertical propagation of stationary waves were proposed by Charney and Drazin (1961), and Eliassen and Palm (1960), there have been many contributions to their development and application in atmospheric sciences. Theoretically, one conventional method employed widely is to assume a simple kind of basic flow separable in vertical and horizontal structures so as to obtain analytical solutions of the problem (see, for example, Charney and Drazin, 1961; Dickinson, 1968, 1980). Based upon numerical models, Matsuno (1970), Schoeberl and Geller (1977) obtained stationary wave solutions with more realistic background flow. In the studies of the horizontal propagation of barotropic waves and the vertical propagation of baroclinic waves under slow varying mean flows, Hoskins and Karoly (1981), and Karoly and Hoskins (1982) derived the equations for wave ray and critical wavenumber similar to the refraction index defined by Matsuno (1970), and obtained conclusions consistant with those from observations and numerical modelling. Based upon a linear stationary-state model with 34 layers in the vertical and adopting climatic zonal mean flow, Huang and Gambo (1983) also found the existence of two vertical wave guides for the propagation of stationary planetary waves, which is in agreement with the findings of Dickinson (1968). All these studies made it evident that the propagation features of stationary waves depend on the structure of the atmospheric zonal flow and the latitude locations. It is therefore possible to understand the kinematic characteristics of th

* Permanent affiliation: Department of Meteorology, Nanjing Institute of Meteorology, Nanjing.

** Laboratory of Numerical Modelling for Atmospheric Sciences and Geophysical Fluid Dynamics.

stationary wave propagation in the atmosphere by analysing the mean basic fields of the atmosphere in different latitudes. To achieve this, in the present study the five-year time mean global general circulation data of Wu and Liu (1987) are employed to investigate the spatial distribution and annual variation of the critical wavenumbers of propagating stationary waves in the troposphere and in the bottom stratosphere. These temporal and spatial variations in the meridional and vertical wave propagations are discussed respectively in Sections II and III and followed by discussions and conclusions.

## II. KINEMATIC CHARACTERISTICS AND ANNUAL VARIATION IN THE MERIDIONAL PROPAGATION OF STATIONARY WAVE

With the refraction theory of Rossby wave, Hoskins and Karoly tackled the problem of meridional wave dispersion by writing the linearized equivalent barotropic vorticity equation in the form of Mercator projection. In the case of conservation and steady state, this becomes

$$[\hat{u}]\frac{\partial}{\partial x}\left(\frac{\partial^2}{\partial x^2}+\frac{\partial^2}{\partial y^2}\right)\psi^* = -\hat{\beta}\frac{\partial\psi^*}{\partial x}, \tag{1}$$

where

$$\begin{cases} x=a\lambda, dy=ad\varphi/\cos\varphi; \\ \hat{u}=\dfrac{u}{\cos\varphi}, \quad \hat{\beta}=\cos\varphi\left(\beta+\dfrac{1}{a}\dfrac{\partial}{\partial\varphi}[\zeta]\right); \\ (u^*,\ v^*)=\left(-\dfrac{1}{a}\dfrac{\partial\psi^*}{\partial\varphi}, \dfrac{1}{a\cos\varphi}\dfrac{\partial\psi^*}{\partial\lambda}\right); \end{cases} \tag{2}$$

other symbols are conventional in meteorology. Letting the solution of perturbation streamfunction be

$$\psi^*=\mathrm{Re}[\tilde{\Psi}(y)\exp(ikx)], \tag{3}$$

and substituting it into Eq. (I) lead to the following amplitude equation

$$\frac{\partial^2\tilde{\Psi}}{\partial y^2}-(k-\hat{\beta}/\hat{u})\tilde{\Psi}=0. \tag{4}$$

Let

$$k_s=(\hat{\beta}/\hat{u})^{1/2}. \tag{5}$$

Then, when

(1) $k>k_s$, the solution is evanescent in the meridional direction

$$\tilde{\Psi}(y)=\exp\{-(k^2-k_s^2)^{1/2}y\};$$

(2) $k<k_s$, there exists wave type solution

$$\tilde{\Psi}(y)=\exp\{i(k_s^2-k^2)^{1/2}y\}.$$

This means that large-scale waves ($k<k_s$) can propagate in the north-south direction whereas small-scale waves ($k>k_s$) are trapped. Thus, a critical wavenumber $n_s=ak_s$ can be defined to distinguish the kinematic differences of different scale stationary waves in their horizontal propagations. According to Eqs. (2) and (5),

$$n_s=a\cos\varphi\left\{\left(\frac{2\Omega}{a}\cos\varphi-\frac{\partial^2[u]}{a^2\partial\varphi^2}+\frac{\partial}{a^2\partial\varphi}[u]\tan\varphi\right)/[u]\right\}^{1/2}. \tag{6}$$

Its square is similar to the barotropic part of the refraction index ($Q_0=[q]_y/[u]$) defined by Matsuno (1970), but with the curvature effect included. This is because for the zonal mean potential vorticity

$$[q]=\nabla^2\psi+f-f_0^2\frac{\partial}{\partial p}\left(\frac{1}{\hat{R}\Theta_p}\frac{\partial\psi}{\partial p}\right), \tag{7}$$

where $\hat{R}=\frac{R}{p}(p/p_0)^{\kappa}$, we have the meridional gradient of its barotropic part

$$a^{-1}[q]_{\varphi}^{\prime r o}=\frac{2\Omega}{a}\cos\varphi-\frac{\partial^2[u]}{a^2\partial\varphi^2}+\frac{\partial}{a^2\partial\varphi}[u]\tan\varphi. \tag{8}$$

Therefore,

$$n_s=a\cos\varphi\{a^{-1}[q]_{\varphi}^{\prime r o}/[u]\}^{1/2}. \tag{9}$$

This critical wavenumber $n_s$ is then determined by geographic latitude, zonal mean westerly and its horizontal shear.

Figs. 1a and 1b show respectively the time-mean distributions of zonal mean westerly and the corresponding gradient of barotropic potential vorticity for the period of December, January and February. The jet centers in the Southern and Northern Hemispheres are respectively located at (45°S, 250hPa) and (32°N, 200 hPa), with the corresponding intensity of 30 m s$^{-1}$ and 42 m s$^{-1}$. Easterly prevails in low latitudes, spanning 60 degrees latitude (30° S—30°N) near the surface and becoming narrower with increasing height. In the stratosphere, the Southern and Northern Hemispheres are dominated respectively by easterly and westerly, with an equatorial easterly maximum located at 15°S. The distribution of the meridional gradient of barotropic potential vorticity (Fig. 1b) is affected by $\beta$-effect and horizontal westerly shear, and overwhelmingly positive with negative sign appearing only in polar areas. The main positive centers are located on the low latitude sides of the upper jet centers near the tropopause, and are particularly strong in the Northern Hemisphere. The isopleths of $n_s$ are very concentrated at the border between easterly and westerly (Fig. 1c), appearing strongly discontinuous. Wave energy may be reflected or absorbed there. The easterly area in low latitudes forms a trapping well which is narrow near the tropopause but very wide in the lower troposphere. Waves can hardly propagate through the trapping area in low layers. Polar areas in the two hemispheres and the lower stratosphere in the Southern Hemisphere are also strong trapping areas. In addition, at 75°S, there is a weak trapping area in the middle and upper troposphere, which is mainly due to the existence of negative value in $[q]_{\varphi}^{\prime r o}$ there.

In the wave propagating area, critical wavenumber decreases poleward generally. At 250 hPa, there are two minimum centers located respectively at 25°N and 50°N, becoming trapping regions for the horizontal propagation of synoptic scale waves. In Fig. 2, the latitudinal distributions of $n_s$ at several heights are given, and the above mentioned features can be observed more obviously. At the high latitudes in the Southern Hemisphere, even planetary waves cannot penetrate the trapping region there. At around (50°N, 300 hPa) in the Northern Hemisphere, there exists a relatively weak trapping region, and waves with wavenumber $n$ more than 3 are trapped easily there, which is in good agreement with the results of Hoskins and Karoly (1981).

In the vertical direction, usually $n_s$ decreases with increasing height in the middle and lower troposphere. From 300 hPa to 100 hPa, the vertical variation of $n_s$ is much smaller. This is mainly due to the fact that the vertical westerly shear is small there ($\partial u/\partial p\approx 0$), and the atmosphere is of equivalent barotropy.

Let us turn to investigating the annual variation of the kinematic characteristics in the wave propagation. For the sake of comparison, we present firstly in Figs. 3a and 3b the

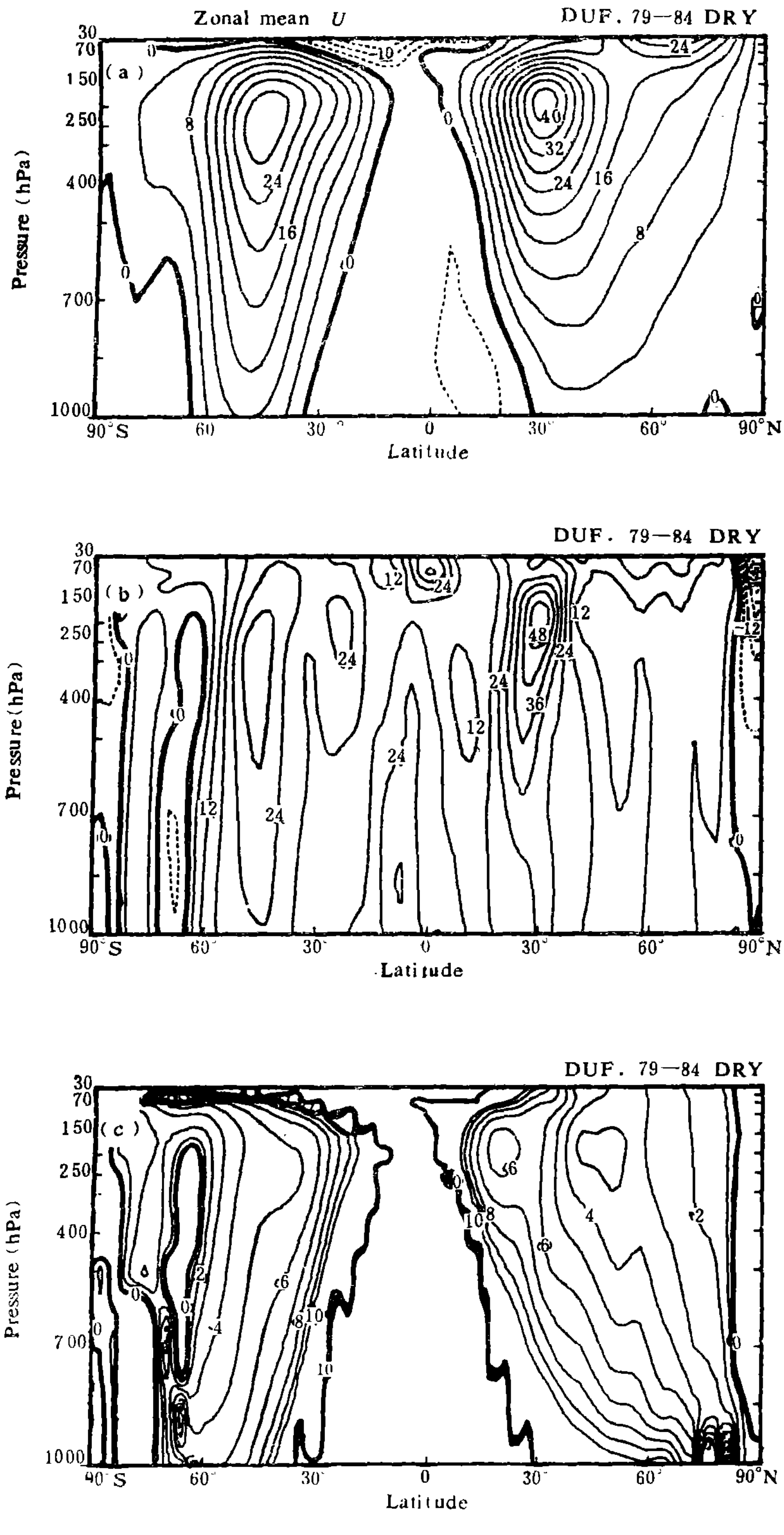


Fig. 1. Zonal mean cross-sections in December, January and February. (a) Zonal mean westerly $[u]$, intervals in 4 m $s^{-1}$; (b) meridional gradient of barotropic potential vorticity $a^{-1}[q]_{\varphi}^{tro}$, intervals in $6\times10^{-12} s^{-1}m^{-1}$; (c) horizontal critical wavenumber $n_s$, intervals in unity.

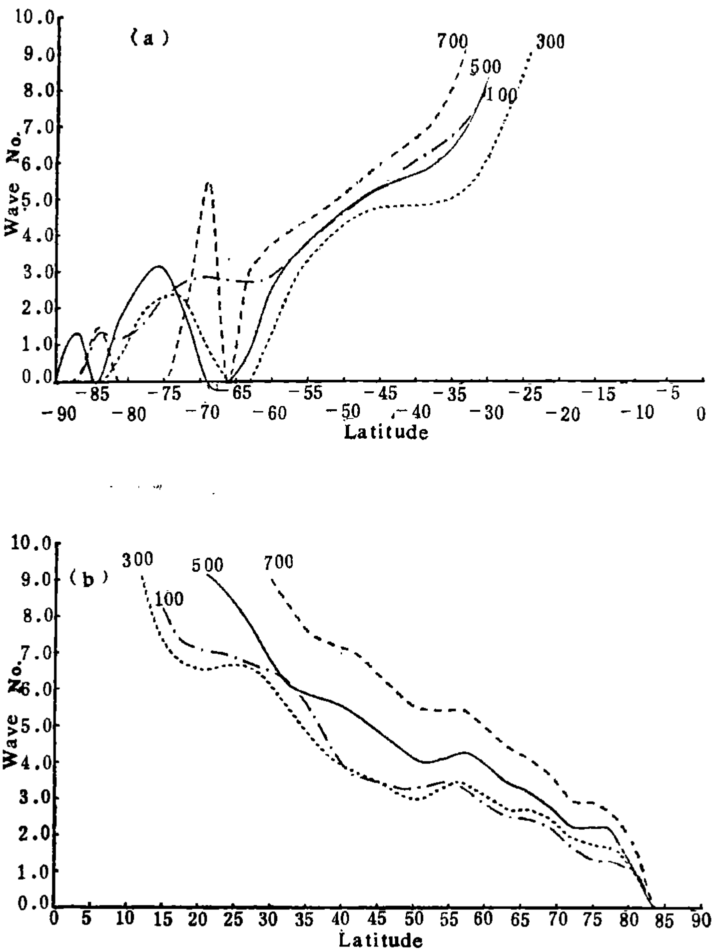


Fig. 2. Latitudinal distributions of the horizontal critical wavenumber $n_s$ at different heights in December, January and February. Dashed, solid, dotted, and dotted-dashed lines denote respectively the distributions at 700, 500, 300 ant 100 hPa.

annual variations of zonal wind $[u]$ at 200 hPa and 500 hPa respectively. At 200 hPa, the strongest westerly is located around 30°, and reaches 46 m s$^{-1}$ in February in the Northern Hemisphere but 37 m s$^{-1}$ in July in the Southern Hemisphere; whereas the strongest equatorial easterly is located at 5°N in the northern hemispheric summer, reaching $-12$ m s$^{-1}$. The annual variation at 500 hPa (Fig. 3b) is quite different from that in the upper troposphere: the strongest westerly centers in the two hemispheres all appear in February, although the southern center is located at higher latitudes. Generally speaking, westerly annual variation in the Northern Hemisphere is stronger than in the Southern Hemisphere. As to the annual varition of $[q]_{\varphi}^{tro}$, it is similar to that presented in Fig. 3a, the maximum centers at 200 hPa are located in the subtropical and midlatitude areas (figures not shown).

Figs. 3c and 3d show the annual variations of $n_s$ respectively at 200 hPa and 500 hPa. The isopleths are generally horizontally distributed. The discontinuity zone in the $n_s$ distribution corresponds to the zero line of $[u]$ very well. Its annual variation in the Northern Hemisphere is stronger than in the Southern Hemisphere, which is closely

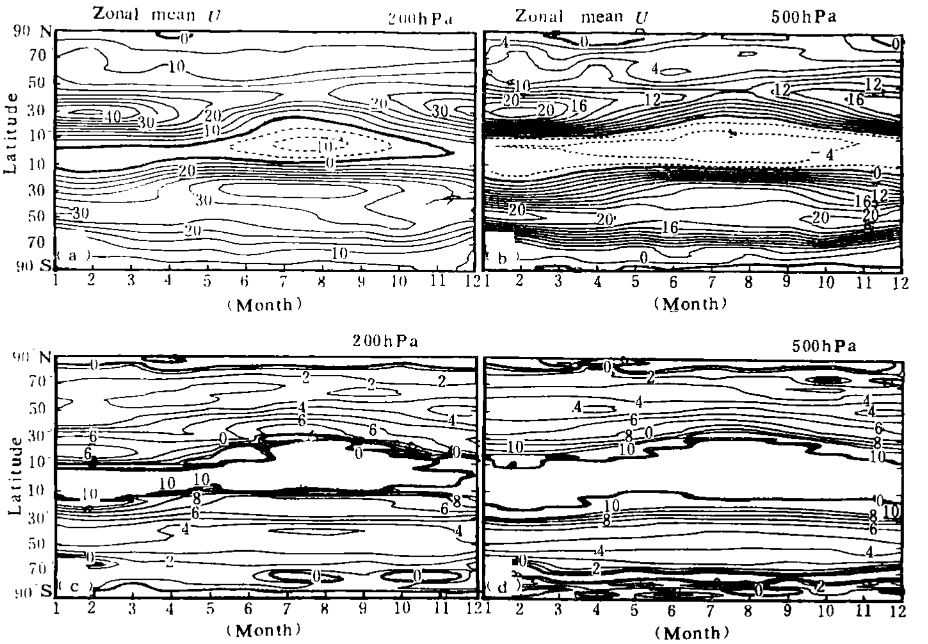


Fig. 3. Annual variations in the latitudinal distributions of zonal mean westerly $[u]$ and critical wave-number $n_s$.
(a) Zonal mean westerly at 200 hPa, intervals in $5\,m\,s^{-1}$;
(b) zonal mean westerly at 500 hPa, intervals in $2\,m\,s^{-1}$;
(c) $n_s$ at 200 hPa, intervals in unity;
(d) $n_s$ at 500 hPa, intervals in unity.

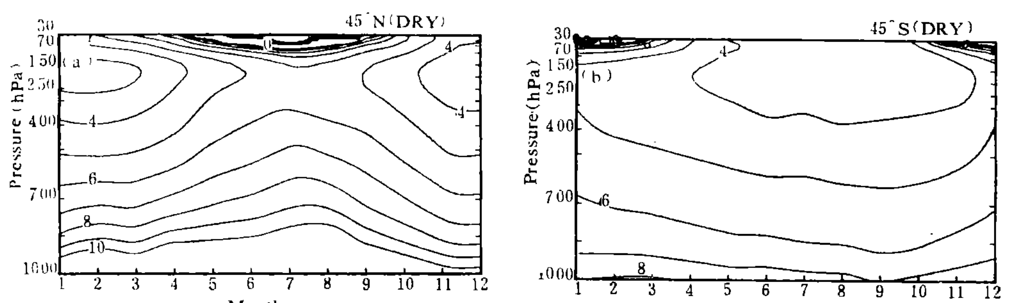


Fig. 4. Annual variations of the vertical distribution of the horizontal critical wavenumber $n_s$ at 45°N (a) and 45° S (b). Intervals in unity.

related to the prominent difference in the annual variation of $[u]$ between the two hemispheres. It can also be seen clearly from these figures that in winter, wave can propagate in lower latitudes, whereas in summer wave propagation is confined to the extratropical areas.

In Fig. 1c, if we make a vertical line at 45°, then the vertical distribution of $n_s$ at this line denotes the vertical distribution of the maximum wavenumber of waves being able to propagate across the latitude 45°. Shown in Fig. 4 is the annual variation of such distribution. At each height in the troposphere, critical wavenumber is small in winter and large in summer. This is in good correspondence with the observed distribution of synoptic systems. In summer in the stratosphere, there exist wave trapping regions. Therefore waves can hardly propagate in the north-south direction. The minimum $n_s$ centers in the two hemispheres are all located at 200 hPa, with the minimum wavenumber 3 appearing in February in the Northern Hemisphere, and 4 in July in the Southern Hemisphere. This implies that in winter in the equivalent barotropic layer between 100 hPa and 300 hPa, only can planetary scale waves propagate freely in the north-south direction. It can also be observed from Fig.4 that synoptic scale waves can propagate arcoss 45° latitude only in the lower troposphere. This is also in good agreement with the fact that synoptic scale baroclinic waves usually develop and propagate in the lower troposphere.

## III. KINEMATIC CHARACTERISTICS AND ANNUAL VARIATION IN THE VERTICAL PROPAGATION OF STATIONARY WAVE

In a steady and conservation system, the linearized eddy potential vorticity equation can be written as

$$[u]\frac{\partial q^*}{\partial x}+v^*\frac{\partial [q]}{a\partial\varphi}=0, \tag{10}$$

where the baroclinic potential vorticity and $q^{\text{cli}}$ barotropic potential vorticity are related by

$$q^{\text{cli}}=q^{\text{tro}}+\frac{f_0}{\rho}\frac{\partial}{\partial z}\left[\frac{\rho}{N^2}\frac{\partial\psi}{\partial z}\right]. \tag{11}$$

Introduce the following kinematic boundary condition

$$w=[u]\frac{\partial h}{\partial x}+a\nabla^2\psi^*, \quad z=0 \tag{12}$$

and let

$$\psi^*=\sin(la\varphi)\,\mathrm{Re}\,(\xi(z)\exp(ikx+z/2H)). \tag{13}$$

Then, after some derivations, the following canonical wave equation can be reached (see for example, Hoskins and Pearce, 1983)

$$\begin{cases}\dfrac{\partial^2\xi}{\partial z^2}-\xi\dfrac{N^2}{f_0^2}(k^2+l^2+r^2-a^{-1}[q]_\varphi/[u])=0,\\[2ex] \dfrac{\partial\xi}{\partial z}+\dfrac{1}{2H}\xi=-\dfrac{N^2}{f_0^2}h,\end{cases} \tag{14}$$

where $h$ is mountain height, $r=f_0/(2HN)$, $z=H\ln(P^*/P)$. If we define a vertical critical wavenumber

$$K_c=a\cos\varphi\,(a^{-1}[q]_\varphi^{\text{cli}}/[u]-f_0^2/4N^2H^2)^{1/2}, \tag{15}$$

then when

$$K=a\cos\phi\,(k^2+l^2)^{1/2}\begin{cases}<K_c\\>K_c\end{cases},\ \xi \text{ possesses}\begin{cases}\text{wave solution,}\\ \text{evanescent solution.}\end{cases} \tag{16}$$

Thus, $K_c$ defined by Eq. (15) can be used to classify the kinematic features in the vertical propagation of different scale waves: waves with total wavenumber $K$ greater than $K_c$ are evanescent in the vertical; whereas planetary scale waves with $K$ less than $K_c$ can propagate in the vertical. Generally the second term $r^2$ within the brackets of Eq. (15) is smaller than the first term. The first term, according to (11),can be separated into barotropic and baroclinic parts. The baroclinic part, which can be expressed as $f_0\ \partial/\partial p(\partial\theta/a\Theta_p\partial\varphi)$, gives approximately the vertical variation of the tilting of isentropic surfaces. It obtains maximum in the strong baroclinic zone in midlatitudes and dominates the magnitude and distribution of $a^{-1}[q]_\varphi^{cli}$. Figs. 5a and 5b show respectively the spatial distributions of $a^{-1}[q]_\varphi^{cli}$ and the critical wavenumber $K_c(z)$ for the vertical wave propagations. The gradient of baroclinic potential vorticity is positive over the whole globe except at the poles and in the lower troposphere at high latitudes. The maximum positive centers are located near the jet centers, i. e. at (30° N, 250 hPa) and (50° S, 350 hPa) with the intensities of $12.5\times10^{-11}$ m$^{-1}$ s$^{-1}$ and $12.1\times10^{-11}$m$^{-1}$s$^{-1}$ respectively. At (75°S, 400 hPa), there is another center of $6.8\times10^{-11}$m$^{-1}$s$^{-1}$. Near the surface there exist strong positive regions too. The northern hemispheric center of $8.9\times10^{-11}$m$^{-1-1}$s is at 45°N, and the southern hemispheric center is at 65° S and weaker.

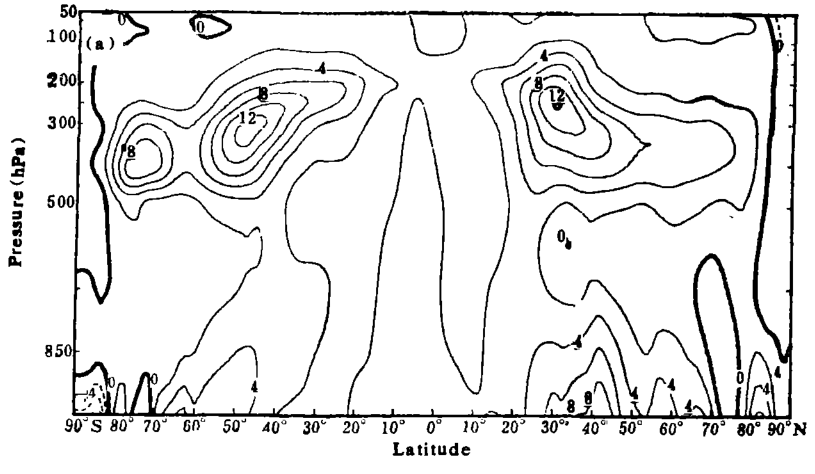


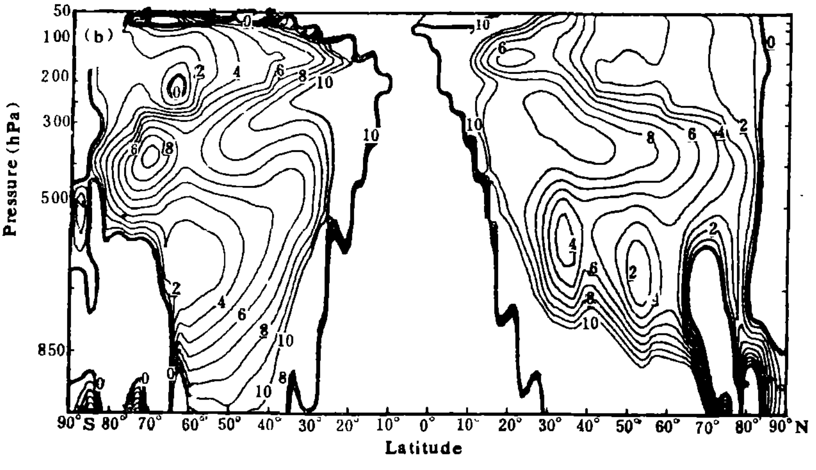


Fig. 5. Spatial distributions of the gradient of baroclinic potential vorticity $a^{-1}[q]_\varphi^{cli}$ (a), and the critical wavenumber $K_c$ for vertically propagating waves (b). Intervals in $2\times10^{-11}$ m$^{-1}$s$^{-1}$ for (a) and in unity for (b).

The locations of the discontinuity belt in the $K_c$ distribution (Fig. 5b) resemble those in the $n_s$ distribution. In the lower troposphere at high latitudes, however, the trapping regions become somewhat wider. This is because in these regions the meridional gradient of baroclinic potential vorticity approaches zero, or even becomes negative. The horizontal variation of $K_c$ also resembles that of $n_s$ in the sense that it generally increases equatorwards. In the vertical, $K_c$ possesses maxima near the surface and in the layer between 400 hPa and 300 hPa, and minima at the tropopause and in the layer between 700hPa and 600 hPa. The altitudes of these centers all decrease with increasing latitudes in the two hemispheres.

In order to see the featues in the vertical wave propagation more clearly, Fig. 6 demonstrates the vertical profiles of $K_c$ at different latitudes. In the midlatitude area in the northern hemispheric winter, vertically propagating waves will meet two trapping regions (Fig. 6a). The first trapping region is near 600 hPa, where $K$ is about 5. Obviously, synoptic scale eddies wil loss substantial part of energy when propagating vertically into this region. The second trapping region is near the tropopause, where $K_c$ is only 3. The near resonant external Rossby waves are trapped here and will become very weak. Thus, only can the planetary scale waves propagate into the stratosphere. In high latitude areas, the wavenumber for upward propagating waves becomes even smaller. In the southern hemispheric summer, the $K_c$ profile at midlatitude (Fig. 6b) is similar to that of the northern hemispheric winter. However, since easterlies dominate the lower stratosphere, waves are mainly confined to within the troposphere.

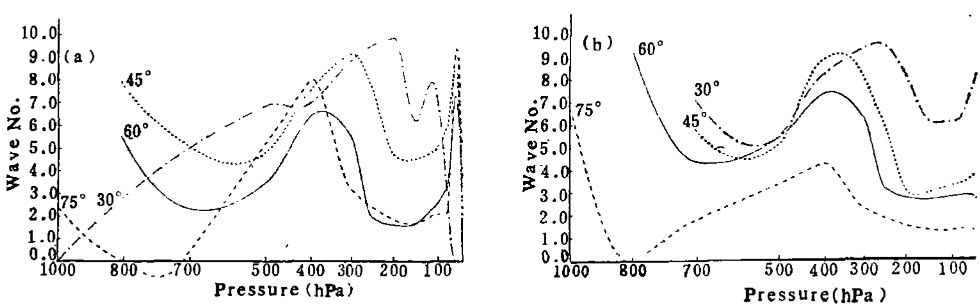


Fig. 6. Vertical profiles of the critical wavenumber $K_c$ at different latitudes in December, January and February. Dashed, solid, dotted and dotted-dashed lines denote respectively the profiles at 75°, 60°, 45° and 30° latitudes. (a) Southern Hemisphere; (b) Northern Hemisphere.

Let us now consider the annual variation of the $K_c$ distributions. Generally speaking, at the height of 300 hPa, there exist good correspondences between the annual variations of $a^{-1}[q]_{\varphi}^{cli}$ and $[u]$, and the annual variation of $K_c$ is mainly determined by that of $a^{-1}[q]_{\varphi}^{cli}$. In Fig. 7 the annual variations of the vertical distribution of $a^{-1}[q]_{\varphi}^{cli}$ at different latitudes are given. At middle and low latitudes, the gradient of potential vorticity in winter possesses maxima near the surface and at the tropopause and minimum in the middle troposphere. In summer in the lower troposphere, it increases with increasing height. It is worthwhile to notice that in the upper troposphere the annual variations of the gradient of baroclinic potential vorticity at 30°and 45° are out of phase. This is mainly due to the seasonal variations in the locations of baroclinic zone and westerly jets, which move equatorwards and locate in the subtropics in winter, and shift back to midlatitudes in summer. At 60° latitudes, the annual variation resembles that in midlatitudes, but is not as obvious as in the upper layer. Another remarkable feature is that in winter such gradient in the bottom troposphere is comparable with that in the upper layer, and even stronger (in the Southern Hemisphere), indicating that the low layer baroclinity in high latitudes in winter is rather strong.

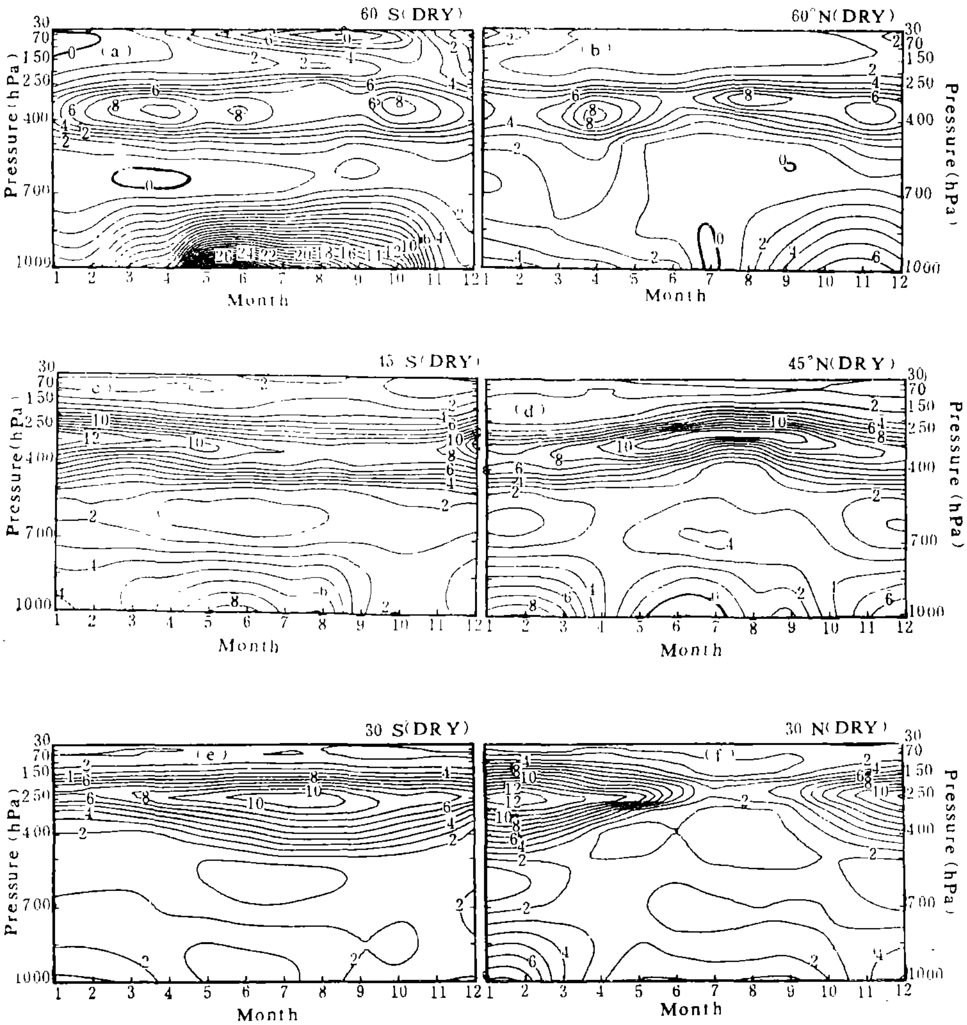


Fig. 7. Annual variations of the horizontal gradient of the baroclinic potential vorticity $a^{-1}[q]_{\varphi}^{c}$ at different latitudes. Units in $10^{-11}$ $m^{-1}s^{-1}$. (a) 60°S; (b) 60° N; (c) 45° S; (d) 45° N; (e) 30°S; (f) 30°N.

Fig. 8 shows the annual variations of the vertical distribution of $K_c$ at different latitudes. The general characteristic is similar to that observed in Fig. 7. In opposition to the winter situation, in summer in the most part of the troposphere $K_c$ is large. Thus, synoptic scale perturbations, once excited, can propagate upwards. However, since in summer, easterlies prevail in the stratosphere, and the tropical easterlies in the lower troposphere also extend northwards, therefore, surface perturbation can hardly penetrate vertically through the easterly layer, neither can perturbations penetrate the tropopause into the stratosphere. In the middle and high latitudes in the Southern Hemisphere, there exists no trapping regions, perturbations can then propagate upwards there. Another important difference between high latitude region and middle and low latitude region is that in the middle troposphere the $K_c$ in high latitudes is greater in winter than in summer. In high latitudes, therefore, upward propagating waves can be easily trapped in summer, but reach high layers in winter. This can, at least partly, explain the observational fact that in winter in high latitudes, smaller scale waves appear quite often at 300 hPa.

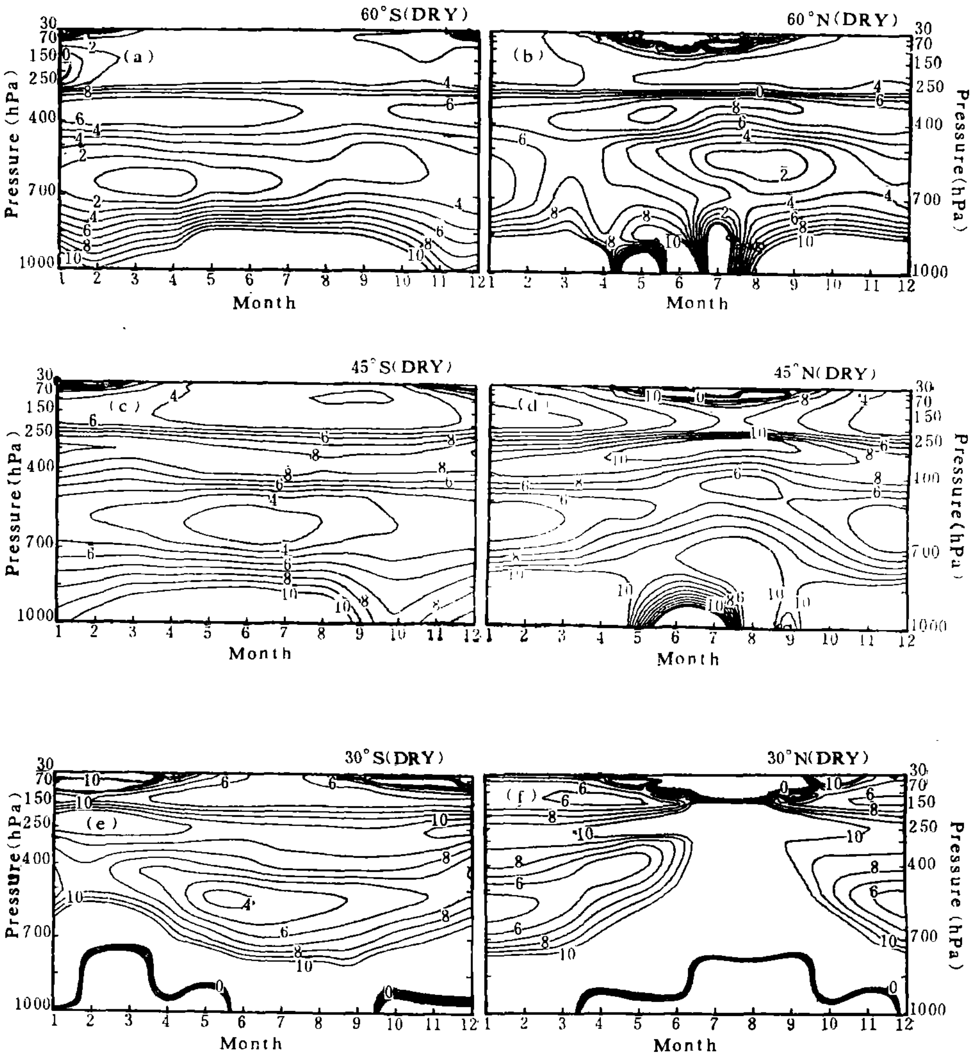


Fig. 8. Annual variations of the critical wavenumber $K_c$ for vertical wave propagation at different latitudes. Interval in unity. (a) 60° S; (b) 60°N; (c) 45°S; (d) 45°N; (e) 30°S; (f)30°N.

## IV. DISCUSSIONS

The kinematic characteristics of the atmospheric wave motion are determined by the earth's curvature and the structures of the atmospheric basic fields including zonal mean westerlies and the meridional gradients of barotropic as well as baroclinic potential vorticity. The meridional gradients of potential vorticity, either barotropic or baroclinic, are also affected substantially by the horizontal and vertical shears of the westerlies. We can therefore conclude that the kinematic characteristics of wave propagation in the earth's atmosphere are determined by the structure of the basic westerlies. These characteristics may thus be described concisely by introducing the horizontal critical wavenumber $n_s$ and the vertical critical wavenumber $K_c$ for wave propagations. Since waves cannot propagate in easterlies, at critical latitudes where zonal westerlies are zero, i. e. the border between easterly and westerly, $n_s$ and $K_c$ are discontinuously distributed. On the easterly side, waves are trapped; whereas on the westerly side, waves even with synoptic scales can propagate freely. Generally, $n_s$ and $K_c$ decrease with increasing latitude as well as altitude. In high latitudes (say 50° N), northward propagating synoptic scale waves are trapped. In the vertical in midlatitudes, there exist two wave trapping regions. The first is at about 600 hPa, waves with total wavenumber $K$ greater than 5 are weakened substantially as they propagate upwards through this region. The second trapping region is near the tropopause where $K_c$ equals 3. The near resonant external Rossby waves propagating upwards from the surface and reaching the tropopause may obtain maximum amplitude there, but strongly weakened further upwards. Therefore, only can planetary scale waves propagate freely into the stratosphere. Due to the prominent difference in the annual variation in zonal mean westerlies between the two hemispheres, the annual variation of $n_s$ in the Northern Hemisphere is stronger than in the Southern Hemisphere. Generally, in winter waves can propagate towards low latitudes, whereas in summer they are confined to middle and high latitudes. The annual variations in the vertical wave propagation are even stronger than in the horizontal wave propagation. Since in summer, easterlies prevail in the stratosphere and invade midlatitudes near the surface, surface perturbation can hardly penetrate surface easterlies upwards, and tropospheric perturbations can hardly propagate into the stratosphere through the tropopause. At high latitudes, the critical wavenumber $K_c$ in the middle troposphere is greater in winter than in summer. Thus smaller scale eddies can propagate upwards into the upper troposphere more easily in winter than in summer. This is in consistence with the fact that in winter at high latitudes, synoptic scale eddies are quite active in the upper troposphere. Therefore, the analyses on the distributions of critical wavenumber for the horizontal as well as vertical propagating waves can help us in understanding the formation of atmospheric perturbations at different latitudes and in different seasons.

Strictly speaking, critical wavenumber as well as refraction index is not the representations of wave behaviour itself, but only a kinematic notation of possible wave behaviour. However, since at the lower boundary of the atmosphere, there always exist thermal and mechanical forcing sources with a variety of scales, then the spatial and temporal distributions of the critical wavenumber as well as refraction index can characterize the corresponding distributions of wave behaviours. This can be supported by comparing the spatial distributions of $n_s$ and $K_c$ with those of the EP-flux. In our parallel research (Wu et al., 1988), we presented the EP-cross-sections in different wavenumber domains. One branch of the upward propagating planetary waves from the surface is refracted towards low latitudes in the upper troposphere. The second branch penetrates the tropopause into the stratosphere. There also exists a weaker branch bending towards high latitudes. These make the EP-flux appearing as "the canopy of coconut tree". On the contrary, the upward synoptic scale EP-flux at middle and high latitudes are all refracted towards low latitudes in the upper troposphere. These are all in good correspondence with the spatial distributions of the critical wavenumbers $n_s$ and $K_c$ which generally decrease with increasing height as well as latitude. In addition, numerical modelling and data analyses both show that synoptic scale eddies dominate the lower troposphere, the near resonant external Rossby waves possess maximum amplitude near the tropopause, and only planetary scale eddies exist in the stratosphere. All these can be well explained by the existence of two wave trapping regions in the $K_c$ profiles at midlatitudes.

The present study only concerns with the zonal maen states. Since westerly structures at different longitudes possess remarkable difference, the three-dimensional wave motion must be much more complicated. For example, local cyclone waves can sometimes propagate upwards into the upper troposphere, and waves in one hemisphere can propagate through the gap of the tropical easterlies into another hemisphere. These cannot be simply described by the two-dimensional critical wavenumbers. It must also be noticed that the theories of horizontal as well as vertical wave propagation upon which the present study was based do not include the impacts of the mean meridional circulation. The recent theoretical study and numerical modelling of Watterson and Schneider (1983) show that the inclusion of the Hadley circulation results in perturbations being able to penetrate the upper tropospheric tropical easterlies and propagate from one hemisphere to the other. There is no doubt that three-dimensional problem is much more difficult but interesting issue, and requires much more efforts. Even so, for the zonal mean climate, and as a basic approximation, the studies on the critical wavenumber $n_s$ and $K_c$ are still of general significance.

This study is partly supported by the National Natural Science Foundation of China under the project number 4860205. The authors are in debt to Ms. Wang Xuan for typing the draft.

## REFERENCES

Charney, J.G. and Drazin, P.G. (1961), Propagation of planetary scale disturbances from the lower into the upper atmosphere, *J. Geophys. Res.*, **66**:83—109.

Dickinson, R.E. (1968), Planetary Rossby waves propagating vertically through weak westerly wind wave guides, *J. Atmos. Sci.*, **25**: 984—1002.

Dickinson, R.E. (1980),Orography effects on planetary flow, GARP publication series, *No.* 23, *W.M.O.*, *Geneva.*

Eliassen, A. and Palm, E. (1960), On the transfer of energy in stationary mountain waves, *Geofys. Publ.*, **22**: No. 3, 1—33.

Hoskins, B.J. and Karoly, D.J. (1981), The steady linear response of a spherical atmosphere to thermal and orography forcing, *J. Atmos. Sci.*, **38**: 1179—1196.

Hoskins, B.J. and Pearce, R. (1983), *Large-Scale Dynamical Processes in the Atmosphere*, Academic Press, New York.

Huang Ronghui and Gambo, K. (1982), The response of a hemispheric multi-level model atmosphere to forcing by topography and stationary heat sources, Part I, II, *J. Meteor. Soc. Japan*, **60**:78—109.

Karoly, D. and Hoskins, B.J. (1982), Three-Dimensional propagation of planetary waves, *J. Met. Soc. Japan*, **60**: 109—123.

Matsuno, T. (1970), Vertical propagation of stationary planetary waves in the winter Northern Hemisphere, *J. Atmos. Sci.*, **27**: 871—883.

Schoeberl, M.R. and Geller, M.A. (1977), A calculation of the structure of stationary planetary waves in winter, *J. Atmos. Sci.*, **34**: 1235—1255.

Watterson, J.G. and Schneider, E.K. (1987), The effect of the Hadley circulation on the meridional propagation of stationary waves, *Quart. J. Roy Meteor. Soc.*, **113**: 779—814.

Wu Guoxiong, Chen Biao and Wu Zhengxian(1988),Moist and dry Eliassen-Palm cross-sections in different wavenumber bands and residual circulation, *Scientia Atmospherica Sinica*, Special Issue, 94—106.

Wu Guoxiong and Liu Huanzhu(1987), *Time-Mean Global General Circulation Statistics*, China Meteorological Press, 212pp.